

Recrystallization Phenomena in Melt-Spun $(\text{Fe}_{100-x}\text{V}_x)_{75}\text{P}_{15}\text{C}_{10}$ Alloys

M. A. S. Karal, K. Bärner, M. Kamruzzaman, D. K. Saha and F. A. Khan

Abstract-- $(\text{Fe}_{100-x}\text{V}_x)_{75}\text{P}_{15}\text{C}_{10}$ ($x=0, 5, 10$ and 15) semi-amorphous alloys were prepared by the melt spinning technique and their structural, thermal and magnetic properties were investigated. The structure of the alloys was studied by X-ray diffraction (XRD) for annealing temperatures of 400°C to 650°C within a 30 minute annealing time. The XRD patterns show that the samples contain a BCC structure for temperatures between 400°C to 450°C and a hexagonal structure for the temperatures between 500°C to 650°C . The lattice parameter of the BCC structure changes from 2.854 to 2.870 \AA with the temperature. The lattice parameters a and c for the hexagonal structure are $(5.011- 5.045) \text{ \AA}$ and $(13.676-13.822) \text{ \AA}$, respectively. The grain size is found to vary from 10 to 60 nm . The recrystallization temperatures of the amorphous phase volume and weight changes were measured by differential thermal analysis (DTA) and thermo gravimetry (TG), respectively. The saturation magnetization gradually decreases with the increase of the substitution of Fe by V at room temperature (RT).

Index Term-- Amorphous alloys; Recrystallization; XRD; DTA; Magnetization

I. INTRODUCTION

Amorphous and nanocrystalline metal alloys are being given special attention in the fields of solid state physics and advanced materials research, particularly regarding their application in electronics and electrical engineering [1-4]. Metallic glasses, which are in a metastable state, can crystallize when heated or held at elevated temperatures for a sufficient time. Crystallization involves a change in properties, such as heat capacity, electrical resistivity, volume and magnetization properties [5]. DTA techniques are the most frequently used method to study the crystallization behavior. However, the reaction needs to occur with a relatively large heat of crystallization and is not very useful when the reaction rate is slow or if only a small heat transfer is involved. The crystallization behavior of metallic glasses has been extensively studied [6, 7]. It may be noted that the DTA measurement allows us to determine the enthalpy difference between an amorphous phase and the crystallized phases by integrating the total area of the exothermic peak upon crystallization. In this study, we will present the structural, thermal and magnetic behavior of a series of as made and annealed $(\text{Fe}_{100-x}\text{V}_x)_{75}\text{P}_{15}\text{C}_{10}$ ($x=0, 5, 10$ and 15) alloys in detail.

M. A. S. Karal is with the Department of Physics, Bangladesh University of Engineering and Technology (BUET), Dhaka-1000, Bangladesh (Corresponding author: Tel.: +880-2-9665650-80 (Ex. 7491), Fax: +880-2-8613046, e-mail: asayem221@phy.buet.ac.bd)

K. Bärner is with the Department of Physics (4 physik), University of Göttingen, F. Hund Platz 1, 37077, Göttingen, Germany (e-mail: k.baerner@t-online.de)

M. Kamruzzaman and F. A. Khan both are with the Department of Physics, BUET, Dhaka-1000, Bangladesh (their e-mails: mkzaman_phybuet@yahoo.com and fakhan@phy.buet.ac.bd)

D. K. Saha is with the Materials Science Division, Atomic Energy Center, Dhaka-1000, Bangladesh (e-mail: dilipbg2001@yahoo.com)

II. EXPERIMENTAL TECHNIQUE

A. XRD measurement

$(\text{Fe}_{100-x}\text{V}_x)_{75}\text{P}_{15}\text{C}_{10}$ ($x=0, 5, 10$ and 15) alloys were prepared by the standard melt spinning technique [8] using a wheel speed of 25 m/sec and a cooling rate of $1.8 \times 10^6 \text{ }^\circ\text{C/sec}$. The ribbon had an average width of $0.75-1.2 \text{ mm}$, a thickness of $10-25 \text{ }\mu\text{m}$ and a length of $2-100 \text{ cm}$. Some ribbons ($10-15$) of the same composition were taken into a crucible and were ground carefully until they became fine power. XRD data were taken of this fine power to check the amorphous nature. The 2θ values revealing both amorphous and crystalline parts were carried out from 30° to 65° using a X'Pert PRO XRD PW 3040 (Phillips) and CuK_α radiation. The average grain size was estimated by the Scherrer analysis, i. e. the XRD peak width. After taking the XRD, the fine power was put in an aluminum foil ($1.5 \text{ cm} \times 1.5 \text{ cm}$) and folded. The foil along with the folded sample was put in a digital furnace (Carbolite, Sheffield, England) at 400°C for 30 minutes. Then the furnace was switched off and allowed to cool to RT. When the furnace had cooled down to RT, the sample was taken out and ground until it became fine powder. The heating and cooling rate of the sample was $10 \text{ }^\circ\text{C/min}$ and $5 \text{ }^\circ\text{C/min}$, respectively. Then the XRD was taken of this fine power. The samples were annealed at 450°C , 500°C , 550°C , 600°C and 650°C for 30 minutes and XRD data were taken in every case. The whole procedure was repeated for the other composition.

B. Grain size measurement

The crystalline grain size of the powder samples was estimated from the broadening of the corresponding X-ray spectral peaks using the Scherrer formula of equation (1).

$$L = \frac{0.9 \times \lambda}{(B - 0.05) \times \cos \theta} \dots \dots \dots (1)$$

where L is the grain size, λ the wavelength of the CuK_α radiation ($\lambda=1.54178 \text{ \AA}$), 0.05 is the instrumentation broadening, B is the full width at half-maximum (FWHM) of a diffraction peak expressed in radians and θ is the Bragg angle.

C. DTA, TG and DTG measurements

The transition temperatures of the samples were monitored by a differential thermal analyzer [Seiko-Ex-STAR-6300, Japan]. The measurements using DTA and TG were carried out from 40°C to 600°C at a heating rate of $20 \text{ }^\circ\text{C/min}$ under nitrogen gas flow. The DTA traces yields the glass transition temperature as determined from the exothermic reaction versus temperature curves. TG provides the weight change in percentage and differential thermo gravimetry (DTG) yields a small change of mass using a small differential thermal reaction.

D. Magnetization measurement at RT

The magnetization was determined using a vibrating sample magnetometer (VSM) at RT and a magnetic field from 0 to 1.172 kG, as described in detail elsewhere [9].

III. RESULTS AND DISCUSSION

A. XRD

Figure 1 show the XRD pattern for as cast samples of the $(\text{Fe}_{100-x}\text{V}_x)_{75}\text{P}_{15}\text{C}_{10}$ alloys ($x=0, 5, 10$ and 15). We have seen that each sample contains a broad peak which confirms the samples are amorphous in nature.

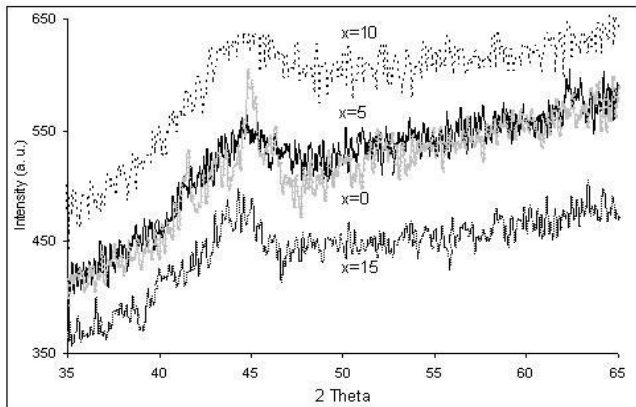


Fig. 1. XRD of as cast sample for $x=0, 5, 10$ and 15

Figures 2, 3, 4 and 5 show the XRD pattern of the alloys of different annealing temperature. The diffraction peaks were identified as (301), (231), (112), (110) and (411) plane at around 35° , 40° , 43° , 45° and 46° for Fe_3P , Fe_3P , Fe_3P , αFe and Fe_3P respectively. Vanadium phosphides are not expected to show clearly as the larger V content is only 15% of the Fe content. The pattern of the samples for temperatures between 400°C and 450°C are consistent with a BCC structure.

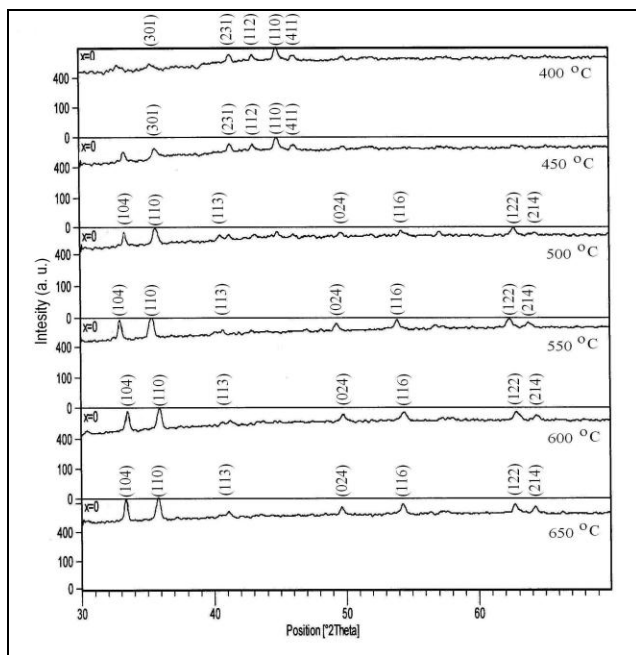


Fig. 2. XRD at different annealing temperature for $x=0$

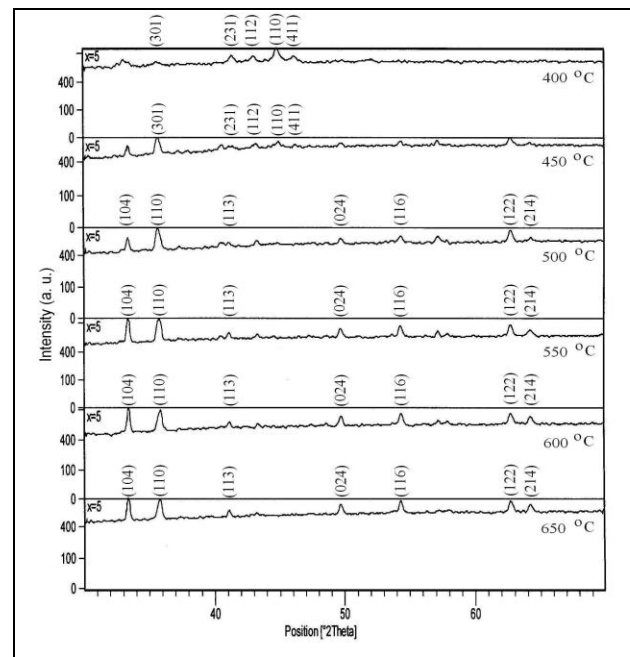


Fig. 3. XRD at different annealing temperature for $x=5$

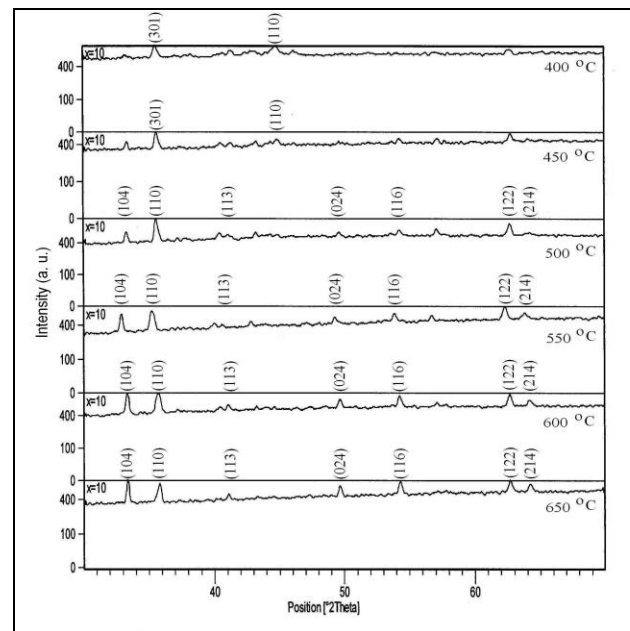


Fig. 4. XRD at different annealing temperature for $x=10$

At 400°C the lattice parameter 'a' of the samples for (110) plane is 2.854 \AA , 2.859 \AA , 2.864 \AA and 2.869 \AA and at 450°C it is 2.852 \AA , 2.854 \AA , 2.857 \AA and 2.857 \AA for $x=0, 5, 10$ and 15 respectively. The increase in lattice parameter and hence the unit cell volume with increasing V content is due to a volume expansion effect as V has the larger atomic radius (1.92 \AA) compared to Fe (1.72 \AA). This behaviour is an agreement with [10]. The linear increase of the lattice parameter of these alloys with increasing V content suggests a simple dilution process. When we increase the temperature from 400°C to 450°C , we observe that the intensity of the (110) plane decreases and simultaneously some new peaks of very low intensity are generated. These new diffraction peaks are identified as (113), (024), (116), (122), (214) and (300) at around 41° , 50° , 54° , 57° , 62° and 64° respectively. The lattice parameter increases with increasing of V content as shown in table I.

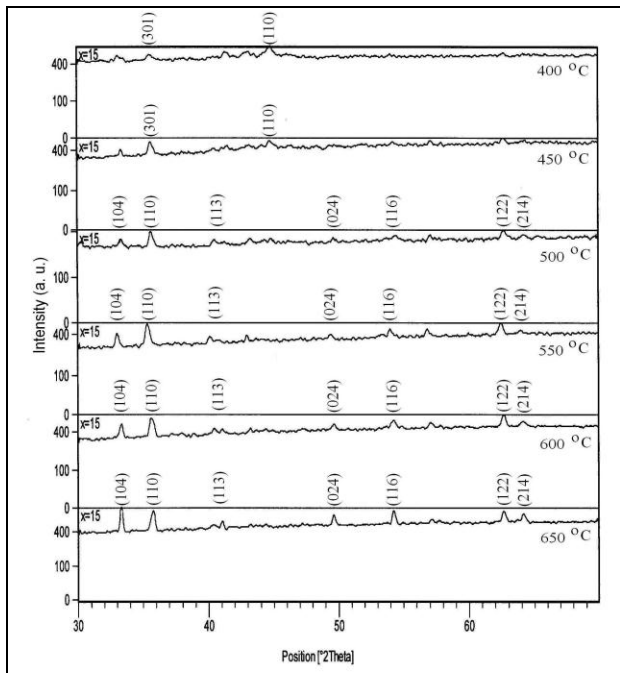


Fig. 5. XRD at different annealing temperature for x=15

TABLE I
LATTICE PARAMETER AND GRAIN SIZE AT DIFFERENT TEMPERATURE FOR
X=0, 5, 10 AND 15

Sample x	Planes (hkl)	Temp. T (°C)	Latt. par. a (Å)	Latt. par. c (Å)	Grain size (nm)
0	110	400	2.854		52
5			2.859		38
10			2.865		32
15			2.870		20
0	110	450	2.853		52
5			2.854		20
10			2.858		28
15			2.858		16
0	116 & 214	500	5.016	13.678	15
5			5.013	13.697	48
10			5.015	13.725	48
15			5.015	13.725	10
0	116 & 214	550	5.040	13.682	40
5			5.018	13.704	48
10			5.045	13.822	48
15			5.027	13.808	48
0	116 & 214	600	5.011	13.676	34
5			5.022	13.682	61
10			5.023	13.709	40
15			5.023	13.707	26
0	116 & 214	650	5.022	13.684	40
5			5.023	13.690	54
10			5.021	13.705	54
15			5.024	13.713	43

From 450 °C to 650 °C these peaks increased in amplitude. This indicates a structural change of the samples from 500 °C to higher temperatures. The structure of these alloys is consistent with a hexagonal structure (JCPDS card No. 80-0042) and with the XRD machine code reference 76-0182. The lattice parameters ('a' and 'c') of this structure were calculated for the planes (116) and (214).

The lattice parameter a is almost constant (~ 5.023 Å) for all samples whereas the lattice parameter c increases linearly with the increase of V content in the temperature range 500 °C to 650 °C as shown in table I. But the lattice parameter c increases from in the range 500 °C to 550 °C and then decreases in the range 600 °C to 650 °C for all the samples, as also shown in table I. At 500 °C the lattice parameter c of the samples taken from the (116) plane is 13.678 Å, 13.697 Å, 13.725 Å and 13.725 Å and at 550 °C it is 13.682 Å, 13.704 Å, 13.803 Å and 13.808 Å for x=0, 5, 10 and 15 respectively. On the other hand, at 600 °C the lattice parameter c from the (116) plane is 13.676 Å, 13.682 Å, 13.709 Å and 13.707 Å and at 650 °C it is 13.684 Å, 13.690 Å, 13.705 Å and 13.713 Å for x=0, 5, 10 and 15, respectively.

B. Grain sizes

The grain size is as small as 10-60 nm in the temperature range 400 °C to 650 °C according to all the peaks shown in table I.

C. DTA, TG and DTG

The DTA, TG% and DTG of the different samples is shown in figures 6, 7, 8 and 9. The crystallization temperature (T_x) increases with the increase of V as shown in figure 10. The peak area of the DTA curve is proportional to the amount of heat released by the material in the amorphous to crystalline or intermediate state reaction at T_x .

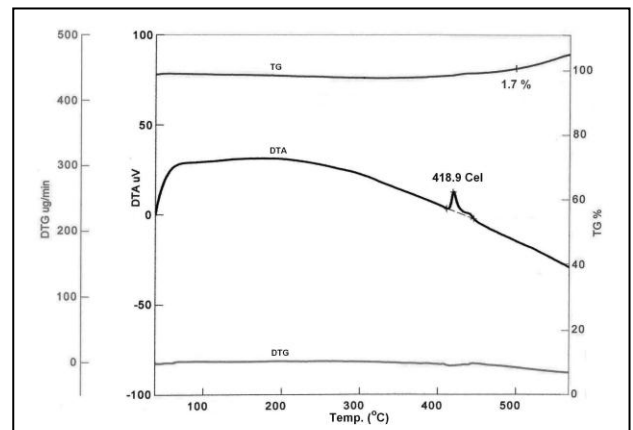


Fig. 6. DTA, TG% and DTG with temperature for x=0

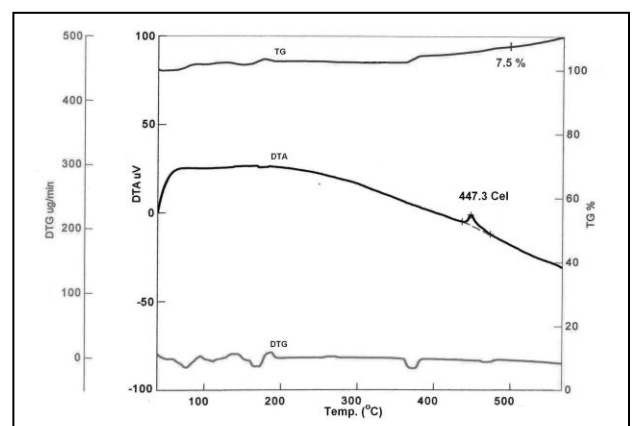


Fig. 7. DTA, TG% and DTG with temperature for x=5

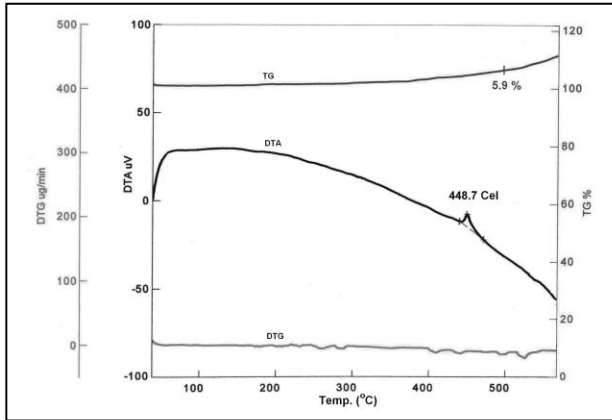


Fig. 8. DTA, TG% and DTG with temperature for x=10

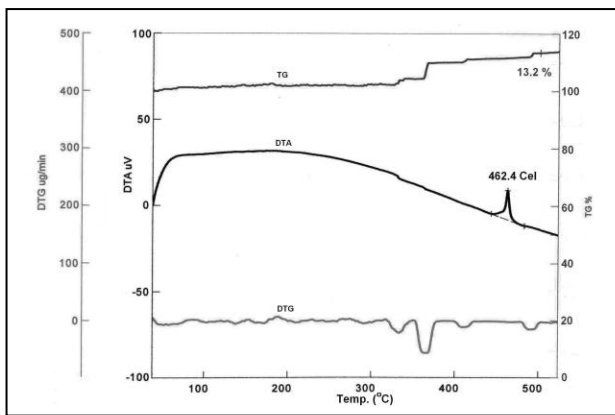


Fig. 9. DTA, TG% and DTG with temperature for x=15

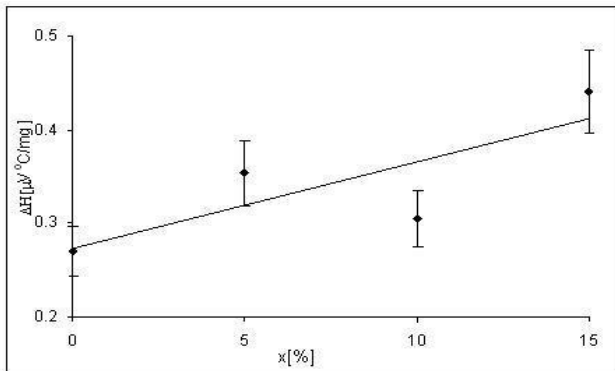


Fig. 10. T_x as a function of x [%]

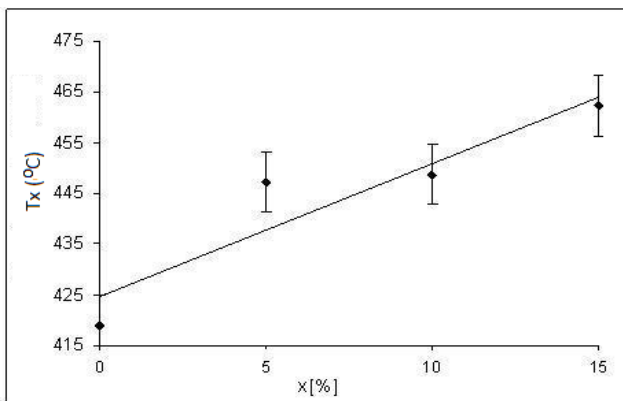


Fig. 11. ΔH as a function of x [%]

Change of enthalpy ΔH is the difference in energy content between the reactant and the products. From figures 10 and 11 we see that both ΔH and T_x vary linearly with composition as expected by Vegard's law. However, the scatter is appreciable and might hide a nonlinear term and so we try for direct correlation between ΔH and T_x which is always possible if we eliminate x .

The empirical quadratic formula follows as:

$$\Delta H = aT_x + bT_x^2 + c \dots\dots\dots (2)$$

where a, b and c are arbitrary constants.

The best fitting values are $a = -0.131067 \mu V/mg$, $b = 0.0001546 \mu V/mg$ and $c = 28.02111 \mu V^\circ C/mg$

We draw the ΔH versus T_x empirical relation by using equation (2) as shown in figure 12. From this figure we find that the curve is not a straight line. So, we conclude that the solid solution is slightly non-ideal i.e., the atoms not distribute completely at random in the alloys.

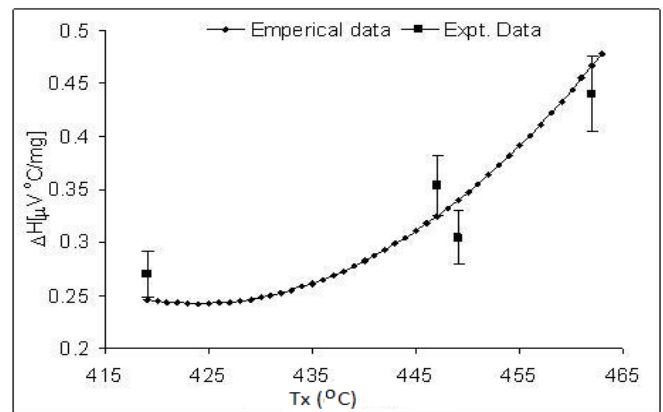


Fig.12 ΔH as a function of T_x

In the TG curve, we observed that the mass is slightly enhanced for all samples. Passively, as the temperature is increased the micro voids which formed during the growth process of the ribbon during melt spinning are gradually eliminated. Then at higher temperatures Fe and V ions absorb oxygen from the environment and hence the mass could be slightly enhanced. The volume/grain increases also with the increase of the V content because the ionic radius of V (1.92 Å) is larger than the ionic radius of Fe (1.72 Å). In the DTG curves some small peaks are found for the samples $x=5$ and 10 which means that there is a small change of mass, but for $x=15$ some broad peaks are found which indicates that there is large change of mass, within small ranges of the heating temperature.

D. Magnetization

When a magnetic field is applied, the magnetic domains align along the field direction and the magnetization saturates, here for relatively low applied fields. The measured values of the saturation magnetization for $x=0, 5, 10$ & 15 were 154, 109, 70 and 40 emu/g respectively. The saturation

magnetization is found to decrease with increasing V content at RT as shown in Fig 13.

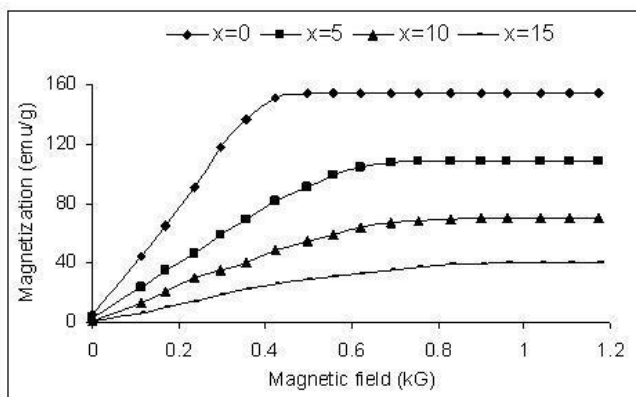


Fig. 13. Magnetization as a function of magnetic field

IV. CONCLUSION

Recrystallization experiments were done on a semi-amorphous Fe-V-P-C series ribbons. The BCC structure is observed for crystallites in the temperature range for 400 °C to 450 °C and the hexagonal structure for temperature 500 °C to 650 °C. The crystalline grain size is found to vary from 10 to 60 nm. The recrystallization temperatures are 418.9 °C, 447.3 °C, 448.7 °C and 462.4 °C for $x=0$, 5, 10 and 15 respectively. The saturation magnetization gradually decreases with increasing V content.

ACKNOWLEDGMENT

International Programme in the Physical Sciences (IPPS), Uppsala is thankfully acknowledged for its support.

REFERENCES

- [1] A. M. Maricic, M. V. Susic, "Correlation of electrical and magnetic permeability with crystallization of glassy iron alloys", *J. Serb. Chem. Soc.*, 56(8/9), 473, 1991
- [2] N. Mitrovic, S. Djukic, A. Maricic, P. Petrovic, A. K. Glisovic, *Science of Sintering: Current problems and new trends*, ed. M. M. Ristic, Belgrade 351, 2003
- [3] N. Mitrovic, R. Simeunovic, A. Maricic, B. Jordovic, "Synthesis, preparation and properties of new Fe-based soft magnetic amorphous alloys with a large supercooled liquid region", *Mater. Sci. Forum*, 453, 2004
- [4] N. E. Cusack: *Amorphous Metals*, IAEA, Wien, 1987
- [5] M.G. Scott, *Amorphous Metallic Alloys*, ed. F.E. Luborsky, Butterworths, London, pp. 144, 1983.
- [6] A. L. Greer, "Pd-Fe interdiffusion in sputtered amorphous alloys" *Acta Metall.*, 30, 171, 1982.
- [7] A. Pratap, K.G. Raval, A. Gupta, S.K. Kulkarni, "Nucleation and growth of a multicomponent metallic glass", *Bull. Mater. Sci.*, 23(3), 185, 2000
- [8] R. C. Budhani, T. C. Goel and K. L. Chopra, "Melt spinning technique for preparation of metallic glasses", *Bull. Mater. Sci.*, 4(5), 549, 1982
- [9] M. Kamruzzaman, M. Phil. Thesis, BUET, 2010
- [10] I. A. Al-Omari, and H. H. Hamdeh, "Mössbauer and structural studies of $\text{Fe}_{0.7-x}\text{V}_x\text{Si}_{0.3}$ alloy system", *Phys. stat. sol. (c)*, 1(7), 1809, 2004